Check for updates

Original Research Article

Therapeutic Potential of Hydroalcoholic Extract of *Rumex alveollatus* L. Leaves in Atherosclerosis: Biochemical, Molecular, and Histopathological Insights from a Rat Model

Pharmacognosy Magazine
22(2) 530–540, 2026
© The Author(s) 2025
Article reuse guidelines:
in.sagepub.com/journals-permissions-india
DOI: 10.1177/09731296251350747
journals.sagepub.com/home/phm
Sage

Bowen Ma[1] and Rui Wang[1]

Abstract

Objectives: Atherosclerosis (AS), a significant cause of cardiovascular diseases, is characterized by disrupted lipid metabolism, inflammation, and endothelial dysfunction. We evaluated the effects and mechanisms of a hydroalcoholic extract from *Rumex alveollatus* L. (RAL) leaves on AS in rats.

Materials and Methods: AS induction was done with a high-fat diet combined with ovalbumin and vitamin D3 injections. Rats were allocated to five groups: normal control, AS model, AS treated with simvastatin, and AS treated with RAL at 300 and 600 mg/kg doses. Treatments were administered intragastrically for 70 days, while controls received water. Key biomarkers, such as total cholesterol (TC), triglycerides (TG), high-density lipoprotein cholesterol (HDL-C), and low-density lipoprotein cholesterol (LDL-C), were analyzed by a biochemistry analyzer. Serum inflammatory markers such as 6-keto-prostaglandin F1α (6-keto-PGF1α), interleukin-1 beta (IL-1β), IL-8, endothelin (ET) thromboxane B2 (TXB2), and nitric oxide (NO) were measured via radioimmunoassay (RIA). Real-time PCR assessed caspase-3, vascular cell adhesion molecule-1 (VCAM-1), and intercellular adhesion molecule-1 (ICAM-1) expression in the thoracic aorta artery.

Results: RAL significantly ($p < .05$) improved lipid profiles by decreasing LDL-C, TC, and TG levels while enhancing HDL-C. It also significantly ($p < .05$) lowered inflammatory cytokines (IL-8 and IL-1β) and caspase-3, ICAM-1, and VCAM-1 gene expression. Additionally, RAL significantly ($p < .05$) enhanced 6-keto-PGF1α and significantly ($p < .05$) increased TXB2 and ET levels. Histopathological analysis revealed reduced liver and arterial damage in AS rats treated with RAL.

Conclusion: These findings suggest that RAL may effectively inhibit AS progression by improving lipid metabolism, reducing inflammation, and protecting endothelial function.

Keywords

Apoptosis, high-fat diet, simvastatin, atherosclerosis, rat, *Rumex alveollatus* L.

Received 07 February 2025; **revised** 09 March 2025; **accepted** 28 March 2025

Introduction

Atherosclerosis (AS) is the main cause of cardiovascular disease (CVD) and stands as the main cause of mortality and disability worldwide. Clinical evidence has established that AS is a precursor to various cardiovascular events, like acute coronary syndrome (ACS) and stroke (Kirwa et al., 2021). Early markers of AS are endothelial dysfunction, disrupted lipid metabolism, and inflammatory responses. Lipids are involved in plaque formation, yet the precise mechanisms linking lipids to AS remain elusive. Observational studies highlight a strong correlation between plasma lipid concentrations and CVD risk (Jebari-Benslaiman et al., 2022; Martinez et al., 2020); AS involves complex cellular and molecular mechanisms, with key processes including lipid accumulation, endothelial dysfunction, oxidative stress (OS), inflammation, and apoptosis. Critical molecules, like vascular cell adhesion molecule-1 (VCAM-1) and intercellular adhesion molecule-1 (ICAM-1), are upregulated against inflammatory cytokines, facilitating leukocyte adhesion and infiltration via nuclear factor kappa-light-chain-enhancer of activated B cells (NF-κB) and reactive oxygen species (ROS)

[1]Department of Cardiovascular Medicine, Xi'an High Tech Hospital, Xi'an, Shaanxi, China

Corresponding author:
Rui Wang, Department of Cardiovascular Medicine, Xi'an High Tech Hospital, Xi'an, Shaanxi 710065, China.
E-mail: wow416106032@sina.com

Creative Commons Non Commercial CC BY-NC: This article is distributed under the terms of the Creative Commons Attribution-NonCommercial 4.0 License (http://www.creativecommons.org/licenses/by-nc/4.0/) which permits non-Commercial use, reproduction and distribution of the work without further permission provided the original work is attributed as specified on the SAGE and Open Access pages (https://us.sagepub.com/en-us/nam/open-access-at-sage).

pathways, thereby driving early plaque formation (Singh et al., 2023). Caspase-3, an effector of apoptosis, contributes to smooth muscle cell and macrophage death, leading to necrotic core formation and plaque instability, with its activation linked to mitochondrial damage and death receptor pathways. Similarly, caspase-6 is implicated in inflammation and late-stage apoptosis (Shan et al., 2021). The balance between thromboxane B2 (TXB2) and prostacyclin (6-keto-prostaglandin F1α), regulated via the cyclooxygenase (COX) pathway, plays a pivotal role in vascular homeostasis, with OS tilting this balance toward thrombosis and endothelial dysfunction (Poznyak et al., 2020; Yu et al., 2022).

Statins are frequently recommended for the treatment of AS because of their ability to lower lipids, reduce inflammation, and protect the endothelium. Nonetheless, they can also be linked to possible side effects and significant expenses (Ali et al., 2021). Combining statins, such as simvastatin, with ezetimibe enhances a decrease in low-density lipoprotein cholesterol (LDL-C) and accelerates lipid-lowering effects. Despite their effectiveness, these therapies have limitations, driving interest toward alternative treatments (Nesti et al., 2020). Natural compounds with lipid-lowering, anti-inflammatory, and antioxidant properties are gaining attention as potential substitutes for statins. Anthocyanins, flavonoids, polyphenols, and other dietary antioxidants are associated with preventing atherogenesis. Additionally, pharmacological studies suggest that certain traditional Chinese medicines (TCMs) exhibit effects comparable to statins, positioning them as promising candidates for AS treatment (Ahmadi et al., 2022).

Rumex alveollatus L. (RAL), a perennial herb from the Polygonaceae family, is rich in bioactive compounds like flavonoids, polyphenols, tannins, and anthraquinones, contributing to its different pharmacological effects (Defaei et al., 2023). Its flavonoids, such as quercetin, apigenin, luteolin, and rutin, exhibit antioxidant and anti-inflammatory effects, reducing OS and supporting vascular health. Preclinical models show anti-diabetic effects, with extracts lowering blood glucose and mitigating high-fat diet (HFD)-induced hyperglycemia (Naseri et al., 2019). Additionally, polyphenols in RAL aid in managing hyperlipidemia and preventing AS by scavenging radicals, inhibiting LDL oxidation, and reducing foam cell formation. Other promising uses include anti-bacterial activity, quorum-sensing inhibition, and selective cytotoxicity against cancer cells (Akbaribazm et al., 2020). We assessed the effects of RAL on experimental AS in rats. This was achieved through an integrated approach, combining biochemical, molecular, and histopathological analyses to elucidate its mechanisms in both preventing and treating AS.

Materials and Methods

Preparation of RAL Hydroalcoholic Extract

The seeds of RAL were collected from Xi'an High-Tech Hospital in Xi'an, China, and identified as RAL leaves by a botanist at the Xi'an Herbarium. The leaves were ground into a fine powder by a soil grinder and homogenized. The crude homogenate was extracted with a water–ethanol solution (30:70 v/v ratio). The resulting extracts were filtered using a No. 40 paper filter and concentrated with a rotary evaporator at 50°C under reduced pressure. The precipitates were collected, freeze–dried, and stored at −20°C until needed for further use (Sadeghi et al., 2019).

AS Induction and Animal Grouping

Fifty adults male Wistar rats, 3 months old (185 ± 15 g), were purchased from Xi'an city animal house and were kept in propylene cages under controlled conditions at 22°C ± 2°C, with a relative humidity of 36% ± 3%, and a light cycle of 12 h of light and 12 h of darkness.

Animals were randomly allocated to 5 groups of 10 animals: normal control, AS model, AS treated with simvastatin, and AS treated with RAL at 300 and 600 mg/kg. The normal group received a standard diet for 70 days, while the other groups received an HFD containing 0.2% pig bile salts, 1% cholesterol, 10% egg yolk powder, 78.8% basal diet, and 10% lard. To induce AS, animals in the AS model, simvastatin-treated and RAL-treated groups were administered 600,000 IU/kg of vitamin D_3 intraperitoneally, followed by subcutaneous injection of ovalbumin (3 mg/kg) mixed with complete Freund's adjuvant on Day 2. The controls received isovolumic saline instead. Starting on Day 10, rats in the treatment groups received daily doses of 300 and 600 mg/kg RAL (AS + 300 and 600 RAL), 10 mg/kg of simvastatin (AS + simvastatin), or water (for the model and normal groups) via intragastric administration for 70 days. At the study's conclusion, after fasting for 12 h, animals were anesthetized with xylazine (100 mg/kg) and ketamine (15 mg/kg), followed by blood sampling by cardiac puncture for serum and plasma analysis. The study followed ethical guidelines set by the ethics committee of Xi'an High-Tech Hospital (Jiang et al., 2017; Naseri et al., 2019; Zhang et al., 2013).

Analysis of Serum Lipid Profile

Serum HDL-C, TC, TG, and LDL-C concentrations were measured by an Automatic Biochemistry Analyzer (GFD-800; Gaomi Caihong Analyzer Co. Ltd., China) following the manufacturer's instructions (Zhang et al., 2013).

Serum Inflammatory Cytokines Analysis

The serum interleukin (IL)-8 and IL-1β concentrations were quantified using radioimmunoassay (RIA) with commercially available kits, following the guidelines. Similarly, the C-reactive protein (CRP) and tumor necrosis factor (TNF)-α levels were evaluated through enzyme-linked immunosorbent assay (ELISA) by commercially provided kits in accordance with the provided protocols (Jiang et al., 2017).

Analysis of Lipid Peroxidation (LPO) and Anti-oxidative Enzyme Activities

LPO in the liver and serum was measured by evaluating the concentrations of thiobarbituric acid-reactive substances (TBARS), considering malondialdehyde (MDA) as a standard, following the procedure by Ohkawa et al. (1979). The enzymatic activities of catalase (CAT), glutathione peroxidase (GSH-Px), and superoxide dismutase (SOD) in both liver and serum were determined using the xanthine oxidase method, a chemical colorimetric method, and the ammonium molybdate method (Naseri et al., 2019), respectively.

Analysis of the Serum ET, Nitric Oxide (NO), 6-keto-PGF1α, and TXB2 Levels

A commercially available kit determined the serum NO concentration as instructed. Plasma 6-keto-prostaglandin F1α (6-keto-PGF1α), endothelin (ET), and TXB2 levels were measured using RIA with commercially supplied kits (Zhang et al., 2013).

Real-time Polymerase Chain Reaction (PCR) Analysis

Total ribonucleic acid (RNA) was obtained from 60 mg of thoracic aorta tissues by adding 1 mL of TRIzol reagent (Catalog No. 12183555; Invitrogen Inc., Lonsee, Germany), followed by a 2-min incubation at 25°C. For complementary deoxyribonucleic acid (cDNA) synthesis, 1,000 ng of total RNA from thoracic aorta tissue was combined with oligo and random primers (1 μL), 10 μL of Takara Bio Mastermix, and 8 μL of deionized water and then subjected to reverse transcription using a thermal cycler (Thermo Fisher Scientific Inc., Lonsee, Germany) with the following protocol: 10 min at 25°C, 45 min at 60°C and 5 min at 60°C. Real-time PCR was conducted using 1 μL each of reverse and forward primers, 1,000 ng of cDNA, and 8 μL of Takara Bio Mastermix using an Applied Biosystems QuantStudio 1 thermocycler (Chicago, US), with 42 cycles of 60°C for 1 min per cycle, followed by melting curve analysis from 60°C to 95°C at a rate of 1°C per second. VCAM-1, ICAM-1, and caspase-3 expression levels were quantified by the $2^{-\Delta\Delta Ct}$ method: $\Delta\Delta Ct = [(Ct_{sample} - Ct_{\beta\text{-actin}}) - (Ct_{control} - Ct_{\beta\text{-actin}})]$ and fold change = $2^{-\Delta\Delta Ct}$. Primer3 software was used to design primers (http://primer3.wi.mit.edu), followed by validating with NCBI Primer-BLAST (https://www.ncbi.nlm.nih.gov/tools/primer-blast/index.cgi), with β-actin considering the internal reference gene. Table 1 provides the primer sequences (Bei et al., 2023).

Table 1. Primer Sequences.

Gene	Sequences (5′-3′)
β-actin	Forward: AGGCATCCTCACCCTGAAGTA Reverse: CACACGCAGCTCATTGTAGA
ICAM-1	Forward: TGGAGAGCAAGAGGACACG Reverse: TCCATGAGGAGGAACATCG
VCAM-1	Forward: GCCAGGAGTATGAGGAAAGG Reverse: TTGGGGTGTTGGTGGTGAG
Caspase-3	Forward: GAGCAAGGAGGAAGTGGA Reverse: CAGTCCAGCAGGAGGAAAG

Note: ICAM-1: Intercellular adhesion molecule-1; VCAM-1: Vascular cell adhesion molecule-1.

ICAM-1, VCAM-1, and Caspase-3 proteins Expression with Western Blotting

Western blotting assessed the VCAM-1, ICAM-1, and caspase-3 protein expression levels. Thoracic aorta tissue samples were homogenized, with 100 mg of tissue mixed with PBS (50 μL) and radio-immunoprecipitation assay (RIPA) buffer (100 μL). After centrifugation, a polyvinylidene fluoride (PVDF) membrane was added with loading buffer (20 μL), which was incubated with primary antibodies against VCAM-1 (Cat # PA5-47029; 100 μg), ICAM-1 (Cat # MA5407; 500 μg) and caspase-3 (Cat # 700182; 100 μg, Thermo Fisher Scientific Inc., Japan). Protein separation was carried out using a 10% SDS-polyacrylamide gel. Following a 12-h incubation at 4°C, the membrane underwent incubation with an HRP-conjugated secondary antibody at 37°C for 40 min. An enhanced chemiluminescence reagent from e-BLOT (China) was applied to visualize protein bands, followed by analysis with Bio-Rad software and further processing in Image J software (Bei et al., 2023).

Histopathological Analysis of Aortic Atherosclerotic Lesions and Hepatic Steatosis

Liver tissue samples and thoracic aortae underwent excision and rinsing with cold saline to isolate any residual blood and debris, ensuring optimal preservation of cellular morphology. The samples were then fixed in 10% formalin for a minimum of 24 h to allow for thorough penetration and stabilization of tissue structures, which is critical for subsequent histological analysis. Following fixation, liver and thoracic aortae sections were cut (thickness: 5 μm) by a microtome, while transverse cross-sections of the aorta were prepared to provide a comprehensive view of the vascular architecture. Both tissue types received hematoxylin and eosin (H&E) staining, a standard technique that highlights cellular components: hematoxylin stains the nuclei blue, providing contrast against the pink-stained cytoplasm and extracellular matrix. Pathological alterations were meticulously assessed under an Olympus optical microscope (BX61TRF; Olympus, Japan), allowing for detailed observation of histological features, like tissue organization, cell morphology, and the presence of any lesions or abnormalities. The intima-media thickness of the aorta was quantitatively assessed using ImageJ software, enabling precise measurement of vascular remodeling and potential pathological changes (Jiang et al., 2017).

Statistical Analyses

Data analyses were performed by SPSS 16.0, utilizing one-way ANOVA and *post hoc* Duncan's test at $p < .05$. The Kolmogorov–Smirnov test evaluated the normality of the data, and $p > .05$ suggested a normal distribution. The values are reported as Mean ± Standard Deviation (SD).

Results

Serum Concentrations of Serum Lipids

In comparison to the controls, the AS group displayed a significant elevation in LDL-C ($p < .01$), TG ($p < .05$), and TC ($p < .01$) serum levels, along with a notable decrease in HDL-C levels ($p < .05$). Conversely, the AS + simvastatin group displayed a significant reduction in these parameters ($p < .05$) when compared to the AS group. The AS + RAL groups displayed a dose-dependent decline in these parameters, along with a dose-dependent elevation in HDL-C levels. The AS + 600 RAL group experienced the most significant improvements in the serum lipid profile, with TG, TC, and LDL-C (all $p < .05$) concentrations significantly reduced, and HDL-C ($p < .05$) levels significantly increased relative to the AS group (Table 2).

Serum Concentrations of Inflammatory Cytokines

In comparison to the normal group, CRP, TNF-α, IL-8, and IL-1β serum concentrations significantly increased in the AS group in of ($p < .01$). In contrast, the AS + simvastatin group exhibited a reduction in the serum concentrations of all four inflammatory cytokines in comparison to the AS group. However, these alterations were not significant ($p > .05$). Animals in the AS + RAL groups displayed a dose-dependent reduction in IL-1β, TNF-α, CRP, and IL-8 concentrations. The most significant reductions in serum inflammatory cytokines were observed in the AS + 600 RAL group, where IL-8 ($p < .05$), TNF-α ($p < .05$), IL-1β ($p < .01$), and CRP ($p < .01$), levels were notably decreased (Table 3).

Serum Levels of LPO and Anti-oxidative Enzyme Activities

Compared to the controls, serum GSH-Px ($p < .05$), T-SOD ($p < .01$), and CAT ($p < .01$) activities significantly decreased in the AS group, and MDA levels were significantly elevated ($p < .05$). In contrast, the AS + simvastatin group exhibited lower MDA concentrations and higher T-SOD, GSH-Px, and CAT activities in comparison to the AS group; however, the alterations were not significant ($p > .05$). Rats in the AS + RAL groups demonstrated a reduction in MDA levels and an elevation in GSH-Px, T-SOD, and CAT activities dose-dependently. The most pronounced improvements were found in the AS + 600 RAL group, where CAT ($p < .05$), GSH-Px ($p < .05$), and T-SOD ($p < .05$), activities were significantly elevated, and serum MDA concentrations ($p < .05$) were significantly decreased versus the AS group (Table 4).

Table 2. Effect of *Rumex alveollatus* L. (RAL) on Serum Lipids (mmol/L).

Group	TC	TG	HDL-C	LDL-C
Normal	1.41 ± 0.4	0.32 ± 0.09	0.91 ± 0.09	0.11 ± 0.01
AS	3.63 ± 0.6##	1.16 ± 0.11#	0.23 ± 0.03#	0.49 ± 0.06##
AS + simvastatin	1.67 ± 0.2*	0.52 ± 0.03*	0.83 ± 0.06*	0.22 ± 0.05*
AS + 300 RAL	2.54 ± 0.2*	0.84 ± 0.06	0.49 ± 0.04	0.36 ± 0.02*
AS + 600 RAL	1.81 ± 0.4**	0.62 ± 0.03*	0.71 ± 0.05*	0.18 ± 0.01**

Notes: Values are Mean ± Standard Deviation (SD), obtained from 10 rats. #$p < .05$, ##$p < .01$, versus the normal group. *$p < .05$, **$p < .01$, versus the atherosclerosis (AS) group. HDL-C: High-density lipoprotein cholesterol; LDL-C: Low-density lipoprotein cholesterol; TC: Total cholesterol; TG: Triglycerides.

Table 3. Effect of *Rumex alveollatus* L. (RAL) on Serum Inflammatory Cytokines.

Group	CRP (ng/L)	TNF-α (ng/L)	IL-8 (ng/mL)	IL-1β (ng/mL)
Normal	4.21 ± 0.6	19.4 ± 1.3	1.91 ± 0.2	0.41 ± 0.06
AS	9.11 ± 0.8##	33.2 ± 2.4##	3.23 ± 0.3##	1.21 ± 0.16##
AS + simvastatin	8.61 ± 0.6	30.6 ± 3.1	3.74 ± 0.6	1.09 ± 0.11
AS + 300 RAL	7.11 ± 0.8*	26.4 ± 2.7	3.11 ± 0.4*	0.81 ± 0.19*
AS + 600 RAL	5.41 ± 0.6**	22.7 ± 2.2*	2.21 ± 0.5*	0.54 ± 0.09**

Notes: Values are Mean ± Standard Deviation (SD), obtained from 10 rats. ##$p < .01$, versus the normal group. *$p < .05$, **$p < .01$, versus the atherosclerosis (AS) group. IL: Interleukin; TNF: Tumor necrosis factor.

Table 4. Effect of *Rumex alveollatus* L. (RAL) on Serum Lipid Peroxidation and Anti-oxidative Enzyme Activity.

Group	T-SOD (U/mL)	GSH-Px (U/mL)	CAT (U/mL)	MDA (nmol/mL)
Normal	149.4 ± 11.2	211.2 ± 14.2	4.92 ± 0.41	4.22 ± 0.25
AS	71.4 ± 9.4##	141.6 ± 12.2#	2.15 ± 0.21##	6.24 ± 0.37#
AS + simvastatin	75.2 ± 10.1	152.3 ± 9.5	2.42 ± 0.34	6.11 ± 0.29
AS + 300 RAL	92.2 ± 10.9	169.1 ± 10.2	3.11 ± 0.32	5.81 ± 0.42
AS + 600 RAL	129.1 ± 12.1*	191.7 ± 9.14*	3.91 ± 0.61*	4.81 ± 0.31*

Notes: Values are Mean ± Standard Deviation (SD), obtained from 10 rats. #$p < .05$, ##$p < .01$, versus the normal group. *$p < .05$, versus the atherosclerosis (AS) group. CAT: Catalase; MDA: Malondialdehyde.

Table 5. Effect of *Rumex alveollatus* L. (RAL) on Serum Concentrations of Nitric Oxide (NO), Endothelin (ET), 6-keto-PGF1α, and Thromboxane B2 (TXB2).

Group	TXB2 (pg/mL)	NO (μmol/L)	ET (pg/mL)	6-keto-PGF1α (pg/mL)
Normal	60.24 ± 9.1	4.71 ± 0.94	171.2 ± 9.1	211.4 ± 14.7
AS	211.4 ± 21.4##	8.11 ± 0.84##	311.6 ± 19.1#	141.2 ± 12.1#
AS + simvastatin	171.2 ± 14.4*	7.91 ± 1.06	232.4 ± 14.2*	161.4 ± 11.4
AS + 300 RAL	122.5 ± 12.9*	5.49 ± 0.85*	206.4 ± 9.4*	151.2 ± 14.2
AS + 600 RAL	81.2 ± 13.2**	4.11 ± 0.74**	161.2 ± 9.1**	189.2 ± 11.2*

Note: Values are Mean ± Standard Deviation (SD), obtained from 10 rats. #$p < .05$, ##$p < .01$, versus the normal group. *$p < .05$, **$p < .01$, versus the atherosclerosis (AS) group.

Serum 6-keto-PGF1α, TXB2NO, and ET Concentrations

In comparison to the controls, the AS group displayed a significant elevation in TXB2 ($p < .01$), NO ($p < .01$), and ET ($p < .05$) serum levels, along with a significant reduction in 6-keto-PGF1α concentrations ($p < .05$). Conversely, the AS + simvastatin group displayed a significant reduction in TXB2 and ET (both $p < .05$) levels in comparison to the AS group. Rats in the AS + RAL groups displayed a dose-dependent decrease in ET, NO, and TXB2 concentrations, along with a dose-dependent increase in 6-keto-PGF1α concentrations. The AS + 600 RAL group showed the most significant improvements, where ET, TXB2, and NO concentrations were significantly decreased ($p < .01$), and serum 6-keto-PGF1α concentrations were significantly increased ($p < .05$) in comparison to the AS group (Table 5).

ICAM-1, Caspase-3, and VCAM-1 Expression

In comparison to the controls, the AS group demonstrated a significant elevation ($p < .01$) in the VCAM-1, ICAM-1, and caspase-3 expression in the thoracic aorta. In contrast, the AS + simvastatin group exhibited a reduction in their expression versus the AS group, although the changes were not significant ($p > .05$). In the RAL-treated groups, a significant decrease in VCAM-1, ICAM-1, and caspase-3 expression were observed, with the most pronounced effects in the AS + 600 RAL group ($p < .01$) and moderate reductions in the AS + 300 RAL group ($p < .05$; Figure 1).

VCAM-1, ICAM-1, and Caspase-3 Protein Expression

Compared to the controls, the VCAM-1, ICAM-1, and caspase-3 expression significantly elevated in the AS group ($p < .01$) in the thoracic aorta. Conversely, the AS + simvastatin group indicated a decrease in their expression relative to the AS group, although such alterations were not significant ($p > .05$). In the RAL-received groups, a notable decrease in VCAM-1, ICAM-1, and caspase-3 expression were observed, with the most significant reductions in the AS + 600 RAL group ($p < .01$) and moderate decreases in the AS + 300 RAL group ($p < .05$) (Figure 2).

Histopathological Alterations in the Thoracic Aorta and Liver

H&E staining examined histopathological alterations in the rat liver (Figure 3) and thoracic aorta (Figure 4). No histopathological alterations were detected in the liver in the normal group using optical microscopy. As shown in Figure 3, in the AS group, severe hepatic steatosis was evident, characterized by hepatocyte apoptosis, shrinkage, and the loss of the normal hexagonal structure of hepatic lobules. Fat vacuoles, lymphatic infiltration (LI), hepatic steatosis, and apoptotic regions were prominent in hepatocytes and portal triad space. In the AS + simvastatin group, the severity of hepatic steatosis was reduced; however, fat vacuoles persisted in hepatocytes, and the hepatic lobular structure remained poorly defined. In the RAL-treated groups (AS + 300 and

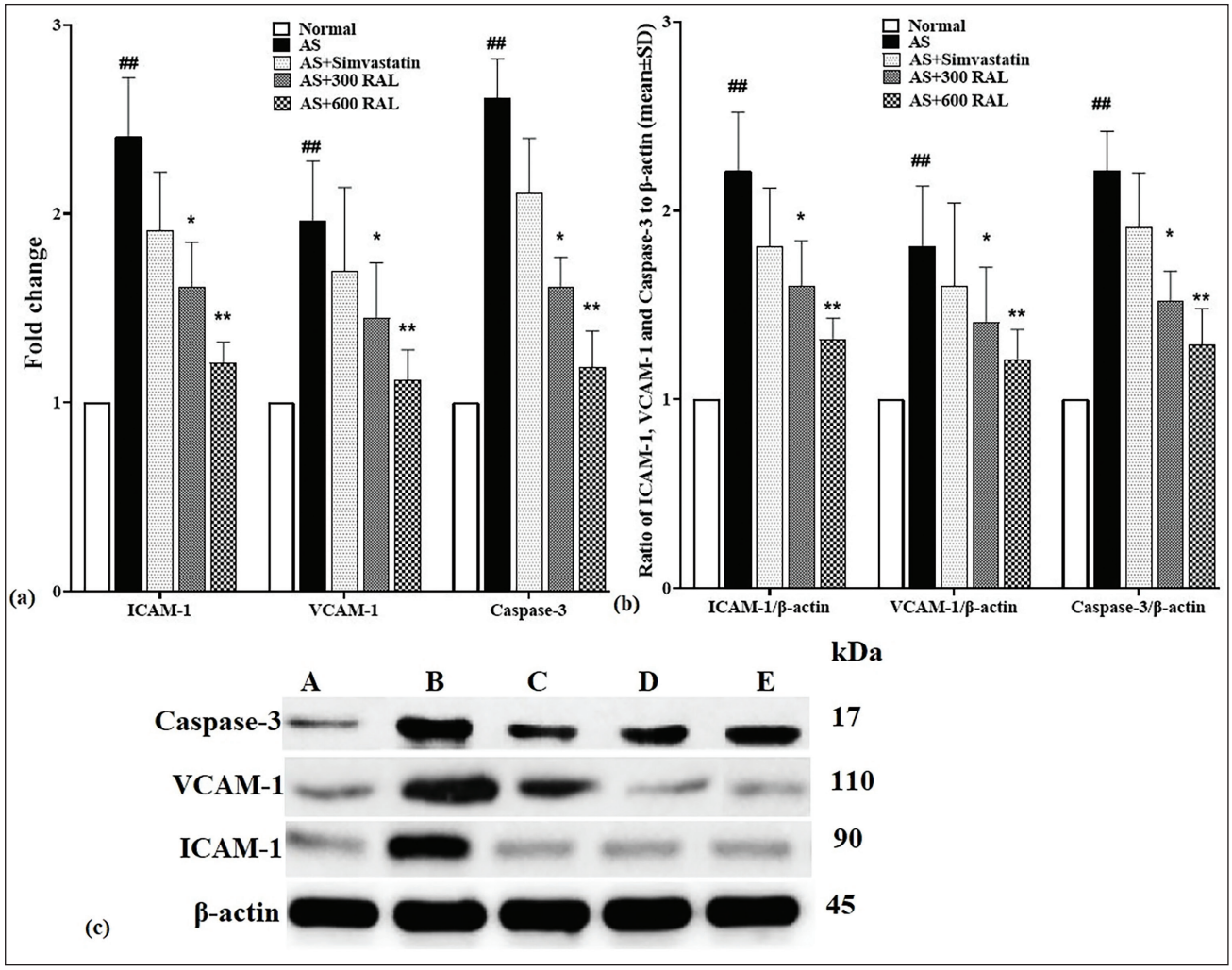


Figure 1. (a) Effect of *Rumex alveollatus* L. (RAL) on Thoracic Aorta Intercellular Adhesion Molecule-1 (ICAM-1), Vascular Cell Adhesion Molecule-1 (VCAM-1) and Caspase-3 Genes Expression. (b) Effect of RAL on Thoracic Aorta ICAM-1, VCAM-1, and Caspase-3 Protein Expression.

Note: Values are Mean ± Standard Deviation (SD), obtained from 10 rats. $^{\#}p < .05$, $^{\#\#}p < .01$, versus the normal group. $^{*}p < .05$, $^{**}p < .01$, versus the atherosclerosis (AS) group.

AS + 600 RAL), a dose-dependent reduction in fat vacuoles and LI in the portal triad space was observed. Moreover, the hepatic lobules regained their normal structure, reflecting the restoration of hepatocyte physiological function. According to Figure 4, the thoracic aorta in the normal group exhibited a healthy vascular structure with normal wall thickness and a smooth endothelial lining without any histopathological abnormalities. In contrast, the AS group displayed notable changes, including thickened and irregular vessel walls with areas of endothelial cell detachment. The elastic fiber plates in the media and intima layers were injured, and extensive atherosclerotic plaques, including cholesterol crystals, foam cells, and calcified tissue, were evident. In comparison to the AS group, the AS + 300 RAL, AS + 600 RAL, and AS + simvastatin groups demonstrated a notable decrease in pathological alterations. Although the vascular walls remained slightly thickened and rough, there were fewer atherosclerotic plaques, and the thoracic aorta structure appeared closer to normal. To assess these changes, the thoracic aorta intima-media thickness was measured. In the AS group, the intima-media thickness ratio (0.74 ± 0.06) was significantly greater compared to the thickness of the controls (0.32 ± 0.04). RAL treatment caused a dose-dependent decrease in this ratio, with the AS + 300 RAL group showing a ratio of 0.51 ± 0.04 and the AS + 600 RAL group displaying a ratio of 0.41 ± 0.03 (both $p < .05$ vs. the AS group). In the AS + simvastatin group, the ratio (0.69 ± 0.04) was slightly lower than the AS group but showed no significant variation ($p > .05$).

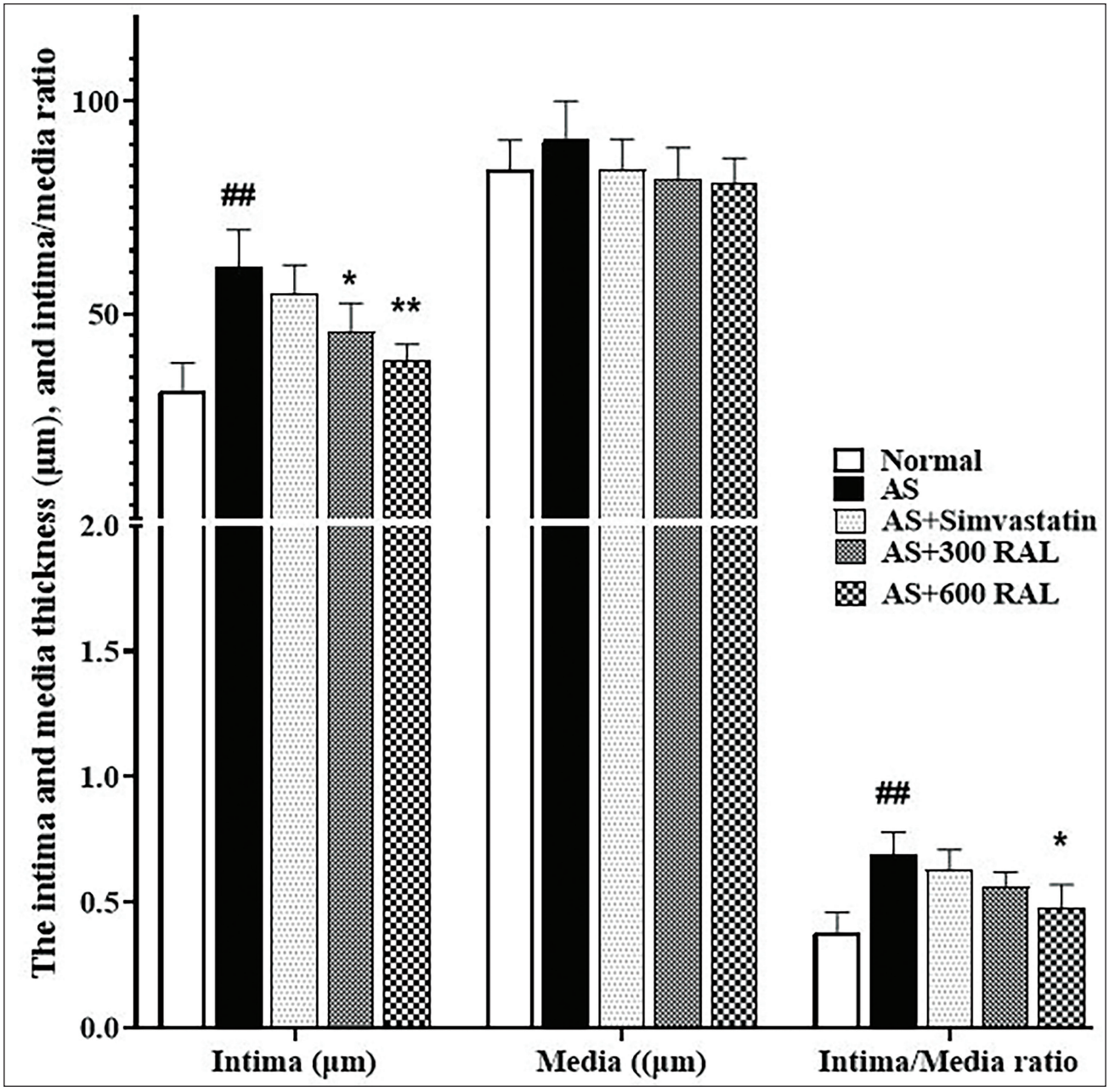


Figure 2. Effect of *Rumex alveollatus* L. (RAL) on Thoracic Aorta Intima and Media Thickness Along with Intima/Media Thickness Ratio.

Note: Values are Mean ± Standard Deviation (SD), obtained from 10 rats. ##$p < .01$, versus the normal group. *$p < .05$, **$p < .01$, versus the atherosclerosis (AS) group.

Discussion

Hyperlipidemia, inflammation, and OS are widely recognized as key factors in the initiation and progression of AS. A rat model of AS was created by feeding an HFD for 70 days, supplemented by excessive vitamin D_3 injections. The rats in the AS group exhibited hyperlipidemia, signs of OS, inflammation, and endothelial dysfunction. The combination of an HFD and calcium overload from high doses of vitamin D_3 led to vascular intimal injury and worsening lipid metabolism abnormalities. Additionally, the HFD OS in the rats resulted in the accumulation of lipid peroxides and a decline in antioxidant enzyme activity. These indicators of hyperlipidemia, endothelial dysfunction, and OS provide a robust model for investigating the anti-atherosclerotic effects of RAL.

In comparison to the AS group, the AS + RAL group was detected with a significant reduction in serum TC, LDL-C, and TG, suggesting that RAL effectively lowers lipid levels in serum and reduces cholesterol deposition in both the liver and the thoracic aorta intima. Elevated LDL-C can

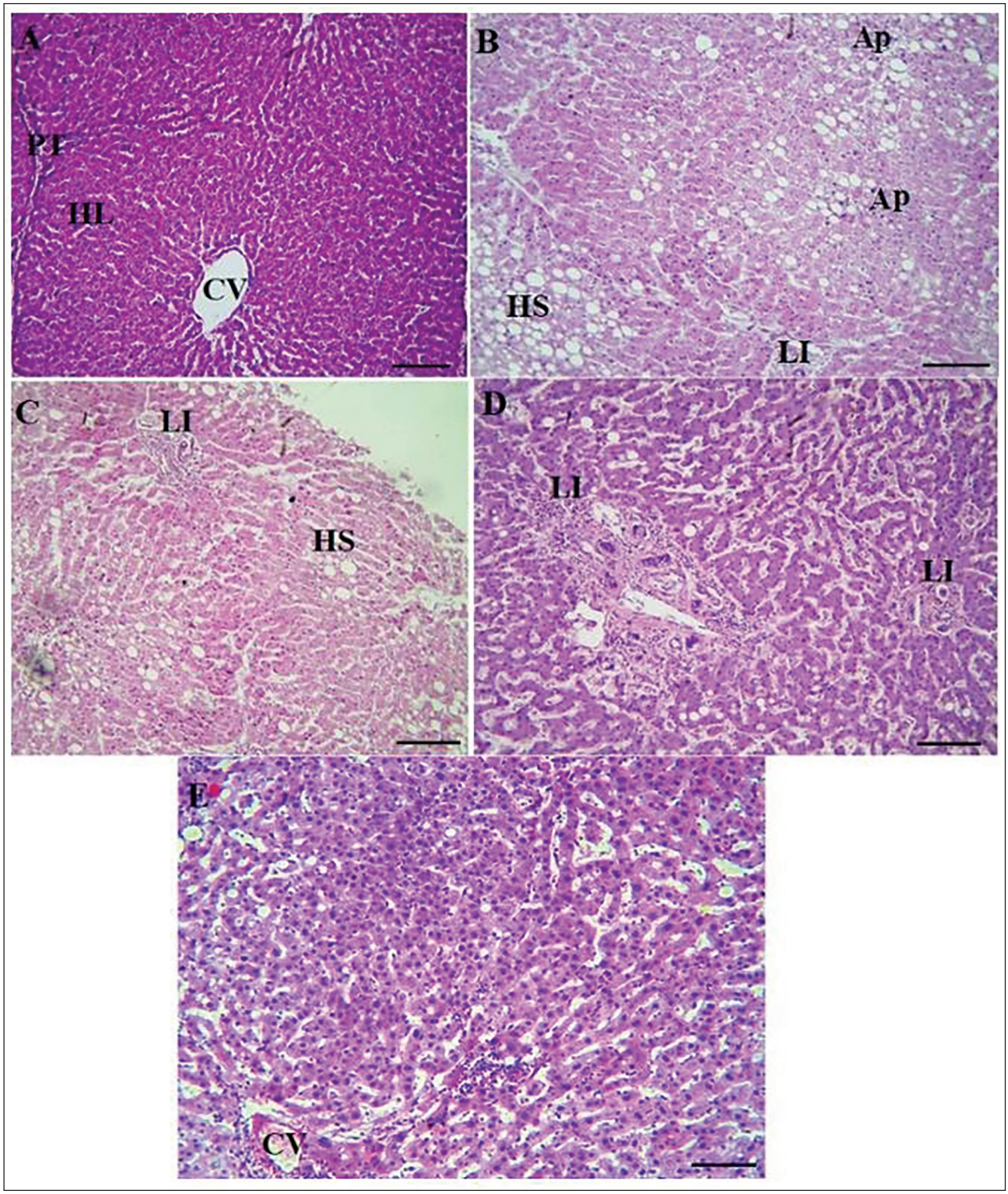


Figure 3. The Histopathological Changes in Liver Tissue in A (Normal), B [Atherosclerosis (AS)], C (AS + Simvastatin), D [AS + 300 *Rumex alveollatus* L. (RAL)], and E (AS + 300 RAL) [Hematoxylin and Eosin (H&E) Staining × 100, Scale Bar = 200 µm].

Note: AP: Apoptotic region; CV: Central venule; HL: Hepatic lobule; HS: Hepatic steatosis; LI: Lymphatic infiltration; PT: Portal triad.

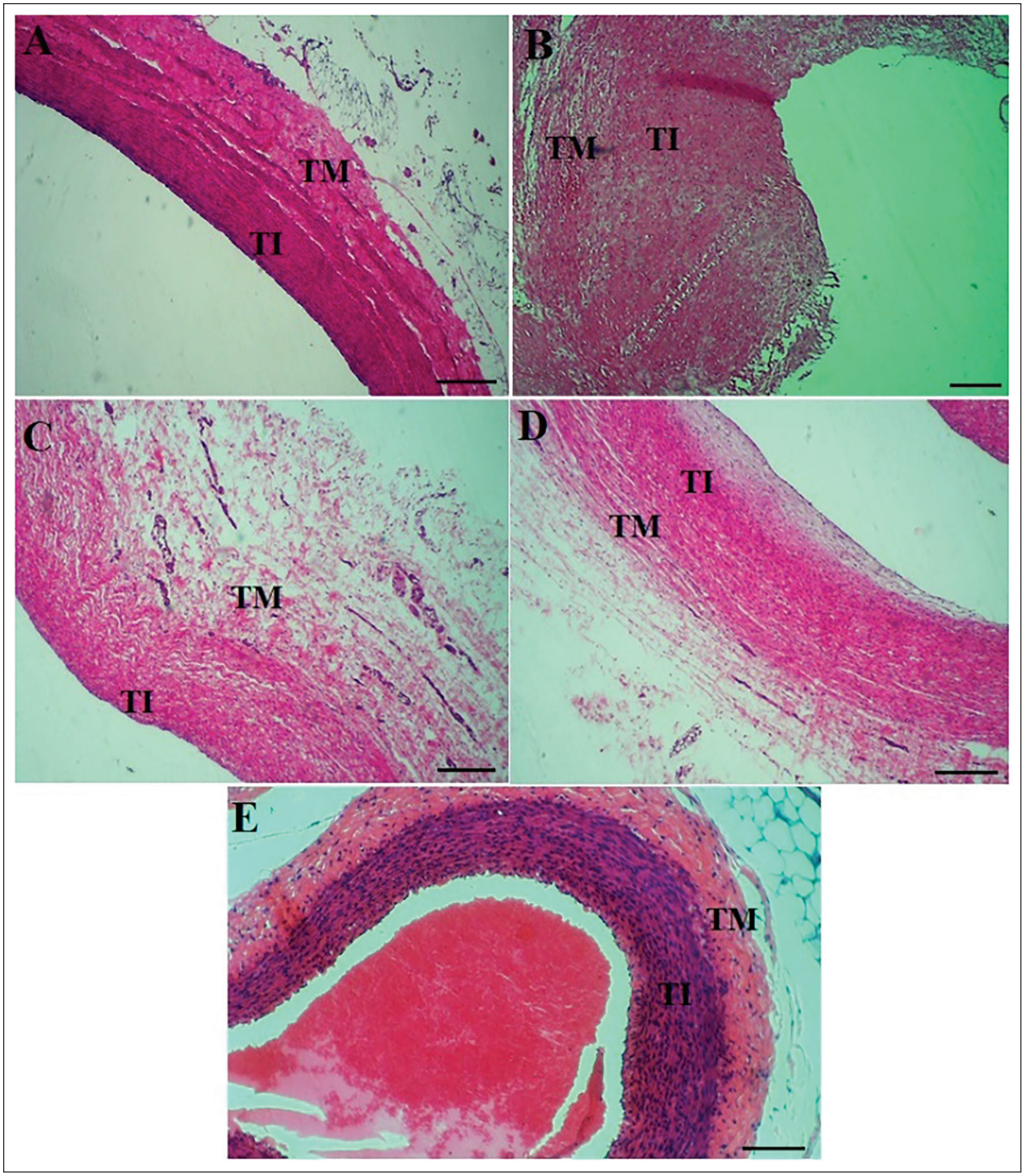


Figure 4. The Histopathological Changes in Thoracic Aorta Tissue in A (Normal), B [Atherosclerosis (AS)], C (AS + Simvastatin), D [AS + 300 *Rumex alveollatus* L. (RAL)], and E (AS + 300 RAL). Tunica Media (TM) and Tunica Intima (TI) [Hematoxylin and Eosin (H&E) Staining × 100, Scale Bar = 200 μm].

accumulate in the vascular wall, leading to plaque formation and arterial lesions (Vekic et al., 2022). RAL's ability to normalize serum LDL-C, TG, and TC levels explains the reduced presence of atherosclerotic plaques in the AS + RAL group. In a study by Naseri et al. (2019), RAL was shown to have hepatoprotective impacts against CCL_4-induced liver damage in mice, improving hepatocyte function by regulating liver enzyme activities (AST, ALT, and ALP) and preserving the normal structure of liver lobules through its antioxidant properties, including reduced NO levels and increased total antioxidant capacity (Naseri et al., 2019). Another research by Sumaira et al. (2017) on *Rumex hastatus* L. leaves found that the plant improved liver profiles (HDL, TC, and LDL) and enhanced serum and liver antioxidant properties in CCL_4-induced hepatotoxicity while regulating liver enzymes (Sumaira Sahreen et al., 2017). In the current study, RAL (particularly at 600 mg/kg) demonstrated a capacity to enhance the activity of endogenous antioxidant enzymes (GSH-Px, T-SOD, and CAT) and significantly reduce LPO levels (MDA). In contrast, simvastatin in the AS + simvastatin group showed limited antioxidant effects and did not significantly alter antioxidant properties.

AS is a chronic inflammatory condition characterized by many important molecules, including CRP (a CVD marker), TNF-α, IL-1β (a vital factor in the AS inflammatory pathway), and IL-8 (crucial for monocyte recruitment). Elevated levels of these markers were found in AS rats (Sinitsky et al., 2020; Tyrrell & Goldstein, 2021). Notably, TNF-α and IL-1β concentrations significantly reduced in the AS + RAL group in comparison to the AS group, and IL-8 levels also dropped significantly with RAL treatment. Thus, RAL's anti-atherosclerotic effects are linked to its ability to suppress inflammatory responses in these rats. Endothelial dysfunction, an early indicator of AS, is associated with 6-keto-PGF1α, NO, ET, and TXB2 levels (Yu et al., 2022). Compared to the controls, the AS group displayed decreased NO and 6-keto-PGF1α levels alongside increased ET and TXB2 levels. After RAL treatment, ET and TXB2 levels decreased while 6-keto-PGF1α levels increased, suggesting that RAL administration benefits AS rats via protecting endothelial function. The RAL is known for its high polyphenol content, with various compounds exhibiting biological effects on cardiovascular health. For instance, rutin and hyperoside enhance coronary flow, while isoquercitrin, chlorogenic acid, rutin, and epicatechin decrease TBARS in Cu^{2+}-related LDL oxidation. Procyanidin B2 inhibits the migration and proliferation of human aortic smooth muscle cells due to advanced glycation end products (Khaliq et al., 2023; Li et al., 2022). These compounds are believed to contribute significantly to the anti-atherosclerotic properties of RAL.

Conclusion

The RAL hydroalcoholic extract significantly slows the progression of AS in rats caused by an HFD and vitamin D_3. RAL treatment notably improved lipid profiles and reduced inflammatory cytokines and liver enzymes, showcasing its anti-inflammatory properties. Additionally, RAL enhanced endothelial function, evidenced by increased serum levels of 6-keto-PGF1α and NO, alongside reductions in ET and TXB2. Thus, RAL has the potential as a natural therapeutic agent for preventing and managing AS due to its lipid-lowering, anti-inflammatory, and endothelial-protective effects. However, the generalizability of these results to humans is limited, necessitating further research through human trials to confirm RAL's efficacy and safety as a therapeutic option for AS.

Abbreviations

ACS: Acute coronary syndrome; AS: Atherosclerosis; CAT: Catalase; CVD: Cardiovascular disease; ELISA: Enzyme-linked immunosorbent assay; ET: Endothelin; GSH-Px: Glutathione peroxidase; HDL-C: High-density lipoprotein cholesterol; HFD: High-fat diet; H&E: Hematoxylin and eosin; ICAM-1: Intercellular adhesion molecule-1; IL: Interleukin; LDL-C: Low-density lipoprotein cholesterol; MDA: Malondialdehyde; NF-κB: Nuclear factor kappa-light-chain-enhancer of activated B cells; NO: Nitric oxide; OS: Oxidative stress; PCR: Polymerase chain reaction; RAL: *Rumex alveollatus* L.; RIA: Radioimmunoassay; ROS: Reactive oxygen species; SOD: Superoxide dismutase; TC: Total cholesterol; TG: Triglycerides; TBARS: Thiobarbituric acid-reactive substances; TXB2: Thromboxane B2; VCAM-1: Vascular cell adhesion molecule-1.

Declaration of Conflicting Interests

The authors declared no potential conflicts of interest with respect to the research, authorship, and/or publication of this article.

Ethical Approval

The experimental protocols of this study were approved by Xi'an High Tech Hospital.

Funding

The authors received no financial support for the research, authorship, and/or publication of this article.

Informed Consent

Not applicable.

ORCID iD

Rui Wang https://orcid.org/0009-0008-1807-9585

References

Ahmadi, A., Jamialahmadi, T., & Sahebkar, A. (2022). Polyphenols and atherosclerosis: A critical review of clinical effects on LDL oxidation. *Pharmacological Research*, *184*, Article 106414. https://doi.org/10.1016/j.phrs.2022.106414

Akbaribazm, M., Khazaei, M. R., & Khazaei, M. (2020). Phytochemicals and antioxidant activity of alcoholic/hydroalcoholic extract of *Trifolium pratense*. *Chinese Herbal Medicines*, *12*(3), 326–335. https://doi.org/10.1016/j.chmed.2020.02.002

Ali, A. H., Younis, N., Abdallah, R., Shaer, F., Dakroub, A., Ayoub, M. A., Iratni, R., Yassine, H. M., Zibara, K., Orekhov, A., El-Yazbi, A. F., & Eid, A. H. (2021). Lipid-lowering therapies for atherosclerosis: Statins, fibrates, ezetimibe and PCSK9 monoclonal antibodies. *Current Medicinal Chemistry*, *28*(36), 7427–7445. https://doi.org/10.2174/0929867328666210222092628

Bei, Y.-R., Zhang, S.-C., Song, Y., Tang, M.-L., Zhang, K.-L., Jiang, M., He, R.-C., Wu, S.-G., Liu, X.-H., Wu, L.-M., Dai, X.-Y., & Hu, Y.-W. (2023). EPSTI1 promotes monocyte adhesion to endothelial cells *in vitro* via upregulating VCAM-1 and ICAM-1 expression. *Acta Pharmacologica Sinica*, *44*(1), 71–80. https://doi.org/10.1038/s41401-022-00923-5

Defaei, A., Karimi, J., & Madani, M. (2023). Environmentally friendly synthesis of silver nanoparticles using *Rumex alveolatus* and their antifungal activity against *Aspergillus niger*. *Biomass Conversion and Biorefinery*, *14*, 32393–32401.

Jebari-Benslaiman, S., Galicia-García, U., Larrea-Sebal, A., Olaetxea, J. R., Alloza, I., Vandenbroeck, K., Benito-Vicente, A., & Martín, C. (2022). Pathophysiology of atherosclerosis. *International Journal of Molecular Sciences*, *23*(6), 3346. https://doi.org/10.3390/ijms23063346

Jiang, Y., Dai, M., Nie, W.-J., Yang, X.-R., & Zeng, X.-C. (2017). Effects of the ethanol extract of black mulberry (*Morus nigra* L.) fruit on experimental atherosclerosis in rats. *Journal of Ethnopharmacology*, *200*, 228–235. https://doi.org/10.1016/j.jep.2017.02.037

Khaliq, T., Akhter, S., Sultan, P., & Hassan, Q. P. (2023). Critical review on *Rumex dentatus* L. a strong pharmacophore and the future medicine: Pharmacology, phytochemical analysis and traditional uses. *Heliyon*, *9*(3), Article e14159. https://doi.org/10.1016/j.heliyon.2023.e14159

Kirwa, K., Szpiro, A. A., Sheppard, L., Sampson, P. D., Wang, M., Keller, J. P., Young, M. T., Kim, S.-Y., Larson, T. V., & Kaufman, J. D. (2021). Fine-Scale air pollution models for epidemiologic research: Insights from approaches developed in the Multi-Ethnic Study of Atherosclerosis and Air Pollution (MESA Air). *Current Environmental Health Reports*, *8*(2), 113–126. https://doi.org/10.1007/s40572-021-00310-y

Li, J.-J., Li, Y.-X., Li, N., Zhu, H.-T., Wang, D., & Zhang, Y.-J. (2022). The genus *Rumex* (Polygonaceae): An ethnobotanical, phytochemical and pharmacological review. *Natural Products and Bioprospecting*, *12*(1), 21. https://doi.org/10.1007/s13659-022-00346-z

Martinez, E., Martorell, J., & Riambau, V. (2020). Review of serum biomarkers in carotid atherosclerosis. *Journal of Vascular Surgery*, *71*(1), 329–341. https://doi.org/10.1016/j.jvs.2019.04.488

Naseri, L., Khazaei, M., Ghanbari, E., & Bazm, M. A. (2019). *Rumex alveollatus* hydroalcoholic extract protects CCL4-induced hepatotoxicity in mice. *Comparative Clinical Pathology*, *28*(2), 557–565. https://doi.org/10.1007/s00580-018-2846-7

Nesti, L., Mengozzi, A., & Natali, A. (2020). Statins, LDL cholesterol control, cardiovascular disease prevention and atherosclerosis progression: A clinical perspective. *American Journal of Cardiovascular Drugs*, *20*(5), 405–412. https://doi.org/10.1007/s40256-019-00391-z

Ohkawa, H., Ohishi, N., & Yagi, K. (1979). Assay for lipid peroxides in animal tissues by thiobarbituric acid reaction. *Analytical Biochemistry, 95*(2), 351–358.

Poznyak, A. V., Grechko, A. V., Orekhova, V. A., Chegodaev, Y. S., Wu, W.-K., & Orekhov, A. N. (2020). Oxidative stress and antioxidants in atherosclerosis development and treatment. *Biology*, *9*(3), 60. https://doi.org/10.3390/biology9030060

Sadeghi, H., Azarmehr, N., Razmkhah, F., Sadeghi, H., Danaei, N., Omidifar, N., Vakilpour, H., Pourghadamyari, H., & Doustimotlagh, A. H. (2019). The hydroalcoholic extract of watercress attenuates protein oxidation, oxidative stress and liver damage after bile duct ligation in rats. *Journal of Cellular Biochemistry*, *120*(9), 14875–14884. https://doi.org/10.1002/jcb.28749

Shan, R., Liu, N., Yan, Y., & Liu, B. (2021). Apoptosis, autophagy and atherosclerosis: Relationships and the role of Hsp27. *Pharmacological Research*, 166, Article 105169. https://doi.org/10.1016/j.phrs.2020.105169

Singh, V., Kaur, R., Kumari, P., Pasricha, C., & Singh, R. (2023). ICAM-1 and VCAM-1: Gatekeepers in various inflammatory and cardiovascular disorders. *Clinica Chimica Acta; International Journal of Clinical Chemistry*, 548, Article 117487. https://doi.org/10.1016/j.cca.2023.117487

Sinitsky, M. Y., Tsepokina, A. V., Kutikhin, A. G., Shishkova, D. K., & Ponasenko, A. V. (2020). Secretion and gene expression of proatherosclerotic cytokines IL6 and IL8 by endothelial cells exposed to mutagen. *Journal of Medical Genetics*, *19*(12), 38–46.

Sumaira Sahreen, S. S., Khan, M. R., & Khan, R. A. (2017). Evaluation of *Rumex hastatus* leaves against hepatic fibrosis: A rat model. *BMC Complementary and Alternative Medicine*, 17, Article 435.

Tyrrell, D. J., & Goldstein, D. R. (2021). Ageing and atherosclerosis: Vascular intrinsic and extrinsic factors and potential role of IL-6. *Nature Reviews. Cardiology*, *18*(1), 58–68. https://doi.org/10.1038/s41569-020-0431-7

Vekic, J., Zeljkovic, A., Cicero, A. F. G., Janez, A., Stoian, A. P., Sonmez, A., & Rizzo, M. (2022). Atherosclerosis development and progression: The role of atherogenic small, dense LDL. *Medicina*, *58*(2), 299. https://doi.org/10.3390/medicina58020299

Yu, L., Liu, H., Ma, X., Seshadri, V. D., & Gao, X. (2022). Anti-atherosclerotic effects of myrtenal in high-fat diet-induced atherosclerosis in rats. *Applied Biochemistry and Biotechnology*, *194*(12), 5717–5733. https://doi.org/10.1007/s12010-022-04044-x

Zhang, J., Liang, R., Wang, L., Yan, R., Hou, R., Gao, S., & Yang, B. (2013). Effects of an aqueous extract of *Crataegus pinnatifida* Bge. var. major NE Br. fruit on experimental atherosclerosis in rats. *Journal of Ethnopharmacology*, *148*(2), 563–569. https://doi.org/10.1016/j.jep.2013.04.053